Supporting Information

Substituents Lead to Differences in the Formation of Two Different Butterfly-shaped $Ni^{II}_2Dy^{III}_2$ Clusters: Structures and Multistep Assembly Mechanisms

Kai-Qiang Mo,[1] Zhong-Hong Zhu,*,[1] Hai-Ling Wang,[1] Xiong-Feng Ma,*,[1] Jin-Mei Peng,[1] Hua-Hong Zou,*,[1] Juan Bai,[1] and Fu-Pei Liang,*,[1]

[1]State Key Laboratory for Chemistry and Molecular Engineering of Medicinal Resources, School of Chemistry & Pharmacy of Guangxi Normal University, Guilin 541004, P. R. China

Table of Contents:

Experimental

Materials and Measurements.

All reagents were obtained from commercial sources and used without further purification. Elemental analyses for C, H and N were performed on a vario MICRO cube. Thermogravimetric analyses (TGA) were conducted in a flow of nitrogen at a heating rate of 5 °C/min using a NETZSCH TG 209 F3 (Figure S1).Powder X-ray diffraction (PXRD) spectra were recorded on either a D8 Advance (Bruker) diffractometer at 293 K (Cu-Kα). The samples were prepared by crushing crystals and the powder placed on a grooved aluminum plate. Diffraction patterns were recorded from 5º to 60º at a rate of 5º min^{-1}. Calculated diffraction patterns of the compounds were generated with the Mercury software (Figure S2).Infrared spectra were recorded by transmission through KBr pellets containing *ca.* 0.5% of the complexes using a PE Spectrum FT-IR spectrometer (400-4,000 cm^{-1}).

Single-crystal X-ray crystallography.

Diffraction data for these complexes were collected on a Bruker SMART CCD diffractometer (Mo Kα radiation and λ= 0.71073 Å) in Φ and ω scan modes. The structures were solved by direct methods, followed by difference Fourier syntheses, and then refined by full-matrix least-squares techniques on F^2 using SHELXL.[1] All other non-hydrogen atoms were refined with anisotropic thermal parameters. Hydrogen atoms were placed at calculated positions and isotropically refined using a riding model. Table S1 summarizes X-ray crystallographic data and refinement details for the complexes. Full details can be found in the CIF files provided in the **Supporting Information**. The CCDC reference numbers are 1947236 (**1**), 1947238 (**2**) and 1947237 (**3**).

[1] Sheldrick, G. M. *Acta Crystallogr., Sect. C: Struct. Chem*. **2015**, *71*, 3-8.

HRESI-MS measurement.

HRESI-MS measurements were conducted at a capillary temperature of 275 °C. Aliquots of the solution were injected into the device at 0.3 mL/h. The mass spectrometer used for the measurements was a ThermoExactive, and the data were collected in positive and negative ion modes. The spectrometer was previously calibrated with the standard tune mix to give a precision of ca. 2 ppm within the region of 100−3,000 *m/z*. The capillary voltage was 50 V, the tube lens voltage was 150 V, and the skimmer voltage was 25 V.

The synthesis method of 1, 2 and 3.

Complex 1: Weighed 0.5 mmol Ni($\mathbf{L^1}$)$_2$ and 0.5 mmol $Dy(NO_3)_2{\cdot}6H_2O$ in 25 mL beaker, and added 12 mL mixed solvent (CH_3OH:CH_3CN = 5:1). Stired for 10 minutes to dissolve. Finally, volatilized at room temperature for 2 days. The aqua crystals was obtained. Yield 36% (Based on Ni($\mathbf{L^1}$)$_2$). IR data for **1** (KBr, cm^{-1}): 3,310 (m), 1,645 (m), 1,461 (s), 1,384 (s), 1,305 (s), 1,216 (s), 1,092 (s), 1,019 (m), 988 (m), 883 (s), 836 (m), 742 (s), 655 (w), 584 (w), 516 (m), 474 (s), 420 (w). Elemental analyses *calc.* (%) for [Dy_2Ni_2($\mathbf{L^1}$)$_4$(CH_3O)$_2$(NO_3)$_4$]: C 32.39, H 3.29, N 7.95. Found: C 32.31, H 3.36, N 7.91.

Complex 2: Weighed 0.5 mmol Ni($\mathbf{L^2}$)$_2$ and 0.5 mmol $Dy(NO_3)_2{\cdot}6H_2O$ in 25 mL beaker, and added 12 mL mixed solvent (CH_3OH:CH_3CN = 5:1). Stired for 10 minutes to dissolve. Finally, volatilized at room temperature for 2 days. The aqua crystals was obtained. Yield 41% (Based on Ni($\mathbf{L^2}$)$_2$). IR data for **2** (KBr, cm^{-1}): 3,318 (m), 1,641 (m), 1,468 (s), 1,380 (s), 1,311 (s), 1,219 (s), 1,096 (s), 1,013 (m), 989 (m), 879 (s), 832 (m), 741 (s), 657 (w), 583 (w), 519 (m), 475 (s), 429 (w). Elemental

analyses *calc.* (%) for $[Dy_2Ni_2(\mathbf{L^2})_4(CH_3O)_2(NO_3)_4]\cdot 2CH_3CN\cdot CH_3OH$: C 35.74, H 4.08, N 8.87. Found: C 35.61, H 4.13, N 8.79.

Complex 3: 0.5 mmol (35.0 mg) NaN_3 was dissolved in 10 mL mixed solvent (CH_3OH:CH_3CN = 5:1) and then immersed in NaN_3 solution with 0.125 mmol (50.2 mg) $Ni(\mathbf{L^2})_2$. After volatilization at room temperature for about two days, the green strip crystal was obtained. Yield 29% (Based on $Ni(\mathbf{L^2})_2$). IR data for **3** (KBr, cm^{-1}): 2,937 (w), 2,031 (s), 1,627 (m), 1,456 (m), 1,306 (m), 1,226 (m), 1,083 (m), 1,024 (m), 904 (w), 743 (m), 634 (w). Elemental analyses *calc.* (%) for $[Ni_2Na_2(\mathbf{L^2})_2(H\mathbf{L^2})_2(N_3)_4]\cdot CH_3OH\cdot H_2O$: C 44.92, H 5.15, N 20.44. Found: C 44.85, H 5.08, N 20.59.

Table S1. Crystallographic data of the complexes **1**, **2** and **3**.

Complex	**1**	**2**	**3**
Formula	$C_{38}H_{40}Dy_2N_8Ni_2O_{22}$	$C_{42}H_{54}Dy_2N_8Ni_2O_{24}$	$C_{40}H_{48}N_{16}Na_2Ni_2O_8$
Formula weight	1403.20	1497.35	1044.15
T (K)	293 (2)	293 (2)	296.15
Crystal system	Monoclinic	Monoclinic	Monoclinic
Space group	$P2_1/c$	$C2/c$	$C2/c$
a (Å)	11.79 (3)	27.760 (6)	24.989 (6)
b (Å)	13.35 (3)	13.880 (3)	11.319 (3)
c (Å)	16.23 (5)	16.570 (3)	20.032 (5)
α (°)	90.00	90.00	90.00
β (°)	110.65 (4)	106.25 (3)	123.044 (3)
γ (°)	90.00	90.00	90.00
V (Å^3)	2390 (12)	6130 (2)	4750 (2)
Z	2	4	4
D_c(g cm^{-3})	1.950	1.623	1.460
μ (mm^{-1})	3.957	3.093	0.879
Reflns coll.	21724	4869	26872
Unique reflns	4446	4869	4645
R_{int}	0.0875	0.000	0.0471
$^aR_1[I \geq 2\sigma(I)]$	0.0771	0.0681	0.0444
$^bwR_2$(all data)	0.2368	0.1946	0.1383
GOF	1.137	1.056	1.081

$^aR_1 = \Sigma||F_o|-|F_c||/\Sigma|F_o|$, $^bwR_2 = [\Sigma w(F_o^2-F_c^2)^2/\Sigma w(F_o^2)^2]^{1/2}$

Table S2. Selected bond lengths (Å) and angles (°) of complexes **1**, **2** and **3**.

1					
Bond lengths (Å)					
Dy1—O2	2.297 (9)	Dy1—O1	2.539 (11)	Ni1—O5	2.032 (8)
Dy1—O5^{i}	2.296 (8)	Dy1—N6^{i}	2.395 (10)	Ni1—O13^{i}	2.097 (8)
Dy1—O13^{i}	2.356 (8)	Dy1—O10	2.484 (11)	Ni1—O13	2.048 (8)
Dy1—O7	2.477 (12)	Dy1—O11	2.433 (11)	Ni1—N3	2.031 (10)
Dy1—O8	2.450 (12)	Ni1—O2	2.018 (8)	Ni1—O4	2.160 (10)
Bond angles (°)					
O2—Dy1—O13^{i}	70.9 (3)	O13^{i}—Dy1—O10	116.8 (3)	O2—Ni1—O5	172.1 (3)
O2—Dy1—O7	154.7 (3)	O13^{i}—Dy1—O11	74.7 (3)	O2—Ni1—O13	104.4 (3)
O2—Dy1—O8	151.4 (3)	O7—Dy1—O1	101.7 (3)	O2—Ni1—O13^{i}	81.9 (4)
O2—Dy1—O1	64.3 (3)	O7—Dy1—O10	66.8 (4)	O2—Ni1—N3	89.2 (4)
O2—Dy1—N6^{i}	88.3 (4)	O8—Dy1—O7	51.4 (3)	O2—Ni1—O4	96.2 (3)
O2—Dy1—O10	122.3 (3)	O8—Dy1—O1	139.9 (3)	O5—Ni1—O13^{i}	94.2 (4)
O2—Dy1—O11	84.1 (3)	O8—Dy1—O10	70.4 (4)	O5—Ni1—O13	81.8 (3)
O2—Dy1—N2	104.1 (3)	O1—Dy1—N2	74.4 (4)	O5—Ni1—O4	77.2 (3)
O5^{i}—Dy1—O2	87.3 (3)	N6^{i}—Dy1—O7	66.4 (4)	O13—Ni1—O13^{i}	82.8 (3)
O5^{i}—Dy1—O13^{i}	70.1 (2)	N6^{i}—Dy1—O8	114.0 (4)	O13—Ni1—O4	158.8 (3)
O5^{i}—Dy1—O7	86.3 (3)	N6^{i}—Dy1—O1	66.0 (4)	O13^{i}—Ni1—O4	95.3 (3)
O5^{i}—Dy1—O8	83.3 (3)	N6^{i}—Dy1—O10	105.9 (4)	N3—Ni1—O5	95.1 (4)
O5^{i}—Dy1—O1	129.0 (3)	N6^{i}—Dy1—O11	141.4 (4)	N3—Ni1—O13^{i}	170.2 (3)
O5^{i}—Dy1—N6^{i}	72.1 (3)	O10—Dy1—O1	71.4 (3)	N3—Ni1—O13	95.4 (4)
O5^{i}—Dy1—O10	150.3 (3)	O10—Dy1—N2	26.3 (3)	N3—Ni1—O4	89.8 (4)
O5^{i}—Dy1—O11	144.7 (3)	O11—Dy1—O7	114.4 (4)	Ni1—O5—Dy1^{i}	104.8 (3)
O13^{i}—Dy1—O7	129.0 (3)	O11—Dy1—O8	88.1 (4)	Ni1^{i}—O13—Dy1^{i}	101.3 (4)
O13^{i}—Dy1—O8	80.6 (4)	O11—Dy1—O1	76.8 (4)	Ni1—O13—Dy1^{i}	102.2 (3)
O13^{i}—Dy1—O1	128.5 (3)	O11—Dy1—O10	50.3 (4)	Ni1—O13—Ni1^{i}	97.2 (3)
O13^{i}—Dy1—N6^{i}	137.3 (3)	O11—Dy1—N2	24.1 (4)		
Symmetry code: (i) -*x*+1, -*y*+1, -*z*+1.					
2					
Bond lengths (Å)					

Dy1—O4^{i}	2.283 (3)	Dy1—O6	2.479 (3)	Ni2—O5	2.130 (3)
Dy1—O1	2.518 (4)	Dy1—O10	2.480 (3)	Ni2—N2	2.105 (4)
Dy1—O9	2.450 (4)	Dy1—O5	2.349 (3)	Ni1—O2	2.012 (3)
Dy1—O2^{i}	2.255 (3)	Dy1—O3	2.508 (3)	Ni1—O5	2.131 (3)
Dy1—O7	2.537 (3)	Ni2—O4	2.066 (3)	Ni1—N1	2.077 (4)
Bond angles (°)					
O4^{i}—Dy1—O1	81.80 (11)	O6—Dy1—O7	50.79 (11)	O4—Ni2—N2^{i}	92.61 (13)
O4^{i}—Dy1—O9	102.30 (11)	O6—Dy1—O10	74.89 (11)	O5—Ni2—O5^{i}	80.47 (19)
O4^{i}—Dy1—O7	147.86 (11)	O6—Dy1—O3	70.17 (11)	N2—Ni2—O5^{i}	161.60 (14)
O4^{i}—Dy1—O6	133.41 (11)	O10—Dy1—O1	137.08 (11)	N2—Ni2—O5	94.81 (14)
O4^{i}—Dy1—O10	140.56 (10)	O10—Dy1—O7	69.12 (11)	N2—Ni2—N2^{i}	94.9 (2)
O4^{i}—Dy1—O5	68.65 (11)	O10—Dy1—O3	119.44 (11)	O2—Ni1—O2^{i}	169.30 (18)
O4^{i}—Dy1—O3	65.38 (10)	O5—Dy1—O1	128.58 (13)	O2—Ni1—O5	90.96 (13)
O1—Dy1—O7	68.03 (11)	O5—Dy1—O9	83.68 (12)	O2—Ni1—O5^{i}	80.83 (13)
O9—Dy1—O1	145.13 (11)	O5—Dy1—O7	122.31 (10)	O2—Ni1—N1	99.06 (13)
O9—Dy1—O7	108.73 (11)	O5—Dy1—O6	152.53 (12)	O2—Ni1—N1^{i}	88.76 (13)
O9—Dy1—O6	75.96 (11)	O5—Dy1—O10	78.08 (11)	O5—Ni1—Dy1^{i}	94.06 (9)
O9—Dy1—O10	52.11 (11)	O5—Dy1—O3	120.79 (11)	O5^{i}—Ni1—O5	80.41 (19)
O9—Dy1—O3	72.10 (11)	O3—Dy1—O1	78.70 (11)	N1—Ni1—O5^{i}	97.41 (14)
O2^{i}—Dy1—O4^{i}	86.58 (11)	O3—Dy1—O7	116.55 (11)	N1—Ni1—O5	169.31 (14)
O2^{i}—Dy1—O1	65.55 (11)	O3—Dy1—N3	92.86 (11)	N1^{i}—Ni1—O5	97.41 (14)
O2^{i}—Dy1—O9	148.49 (10)	O3—Dy1—N4	95.83 (12)	N1^{i}—Ni1—N1	86.6 (2)
O2^{i}—Dy1—O7	71.36 (11)	O4—Ni2—O4^{i}	179.35 (17)	Ni2—O4—Dy1^{i}	109.28 (13)
O2^{i}—Dy1—O6	119.40 (11)	O4—Ni2—O5	103.50 (13)	Ni1—O2—Dy1^{i}	105.64 (13)
O2^{i}—Dy1—O10	102.67 (11)	O4—Ni2—O5^{i}	77.01 (12)	Ni2—O5—Dy1	104.70 (14)
O2^{i}—Dy1—O5	71.39 (11)	O4^{i}—Ni2—O5	77.01 (12)	Ni2—O5—Ni1	99.56 (15)
O2^{i}—Dy1—O3	137.44 (11)	O4—Ni2—N2	86.95 (13)	Ni1—O5—Dy1	98.72 (13)
O6—Dy1—O1	76.51 (12)				
Symmetry code: (i) -*x*+1, *y*, -*z*+1/2.					
3					
Bond lengths (Å)					
Ni1—O1	1.918 (3)	Ni1—N3	1.940 (4)	Na1—O3	2.505 (3)
Ni1—O3	1.938 (3)	Ni1—N6	1.963 (3)	Na1—O3^{i}	2.361 (3)

Ni1—N1	1.938 (4)	Na1—O1	2.301 (3)	Na1—O4^{i}	2.375 (3)
Ni1—N2	1.952 (3)	Na1—O2	2.406 (3)	Na1—N6^{i}	2.467 (4)
Bond angles (°)					
O1—Ni1—O3	86.54 (12)	N2—Ni1—N6	174.43 (15)	O3^{i}—Na1—O3	92.79 (11)
O1—Ni1—N1	93.17 (14)	N3—Ni1—N2	95.20 (16)	O3^{i}—Na1—O4^{i}	68.56 (10)
O1—Ni1—N2	87.43 (14)	N3—Ni1—N6	88.27 (16)	O3^{i}—Na1—N6^{i}	65.27 (11)
O1—Ni1—N3	173.49 (15)	O1—Na1—O2	67.24 (11)	O4^{i}—Na1—O2	116.71 (13)
O1—Ni1—N6	88.66 (14)	O1—Na1—O3	66.59 (10)	O4^{i}—Na1—O3	83.56 (11)
O3—Ni1—N1	174.80 (14)	O1—Na1—O3^{i}	149.62 (12)	O4^{i}—Na1—N6^{i}	130.53 (12)
O3—Ni1—N2	92.02 (13)	O1—Na1—O4^{i}	126.90 (12)	N6^{i}—Na1—O3	115.00 (12)
O3—Ni1—N3	87.41 (16)	O1—Na1—N6^{i}	102.21 (12)	Ni1—O1—Na1	104.15 (12)
O3—Ni1—N6	83.78 (13)	O2—Na1—O3	132.51 (11)	Ni1—O3—Na1	96.52 (11)
N1—Ni1—N2	93.16 (15)	O2—Na1—N6^{i}	85.04 (12)	Ni1—O3—Na1^{i}	107.22 (12)
N1—Ni1—N3	92.63 (18)	O3^{i}—Na1—O2	134.02 (12)	Na1^{i}—O3—Na1	77.69 (10)
N1—Ni1—N6	91.02 (15)				
Symmetry code: (i) -*x*+1, *y*, -*z*+1/2.					

Table S3. Hydrogen-bonds for complexes **1**, **2** and **3**.

1		
Hydrogen bond	**Distance[a], Å**	**Angle[b], °**
C_1–H_{1C}···O_8	2.510	137
C_{14}–H_{14}···O_{12}	2.549	156
2		
Hydrogen bond	**Distance[a], Å**	**Angle[b], °**
C_2–H_{2B}···O_8	2.512	132
C_5–H_5···O_8	2.484	143
C_{12}–H_{12A}···O_8	2.543	150
C_{19}–H_{19}···O_9	2.575	168
3		
Hydrogen bond	**Distance[a], Å**	**Angle[b], °**
C_8–H_{8B}···N_5	2.459	149

[a] Distance between acceptor and donor; [b] Angle of acceptor–hydrogen–donor.

Table S4. *SHAPE* analysis of the Dy1 ion in **1**.

Label	Shape	Symmetry	Distortion(°)
EP-9	D_{9h}	Enneagon	36.266
OPY-9	C_{8v}	Octagonal pyramid	21.672
HBPY-9	D_{7h}	Heptagonal bipyramid	17.276
JTC-9	C_{3v}	Johnson triangular cupola J3	15.769
JCCU-9	C_{4v}	Capped cube J8	6.566
CCU-9	C_{4v}	Spherical-relaxed capped cube	4.765
JCSAPR-9	C_{4v}	Capped square antiprism J10	3.750
CSAPR-9	C_{4v}	Spherical capped square antiprism	2.572
JTCTPR-9	D_{3h}	Tricapped trigonal prism J51	5.238
TCTPR-9	D_{3h}	Spherical tricapped trigonal prism	3.146
JTDIC-9	C_{3v}	Tridiminished icosahedron J63	11.035
HH-9	C_{2v}	Hula-hoop	9.847
MFF-9	C_s	Muffin	2.920

Table S5. *SHAPE* analysis of the Dy1 ion in **2**.

Label	Shape	Symmetry	Distortion(°)
EP-9	D_{9h}	Enneagon	35.042
OPY-9	C_{8v}	Octagonal pyramid	19.979
HBPY-9	D_{7h}	Heptagonal bipyramid	16.112
JTC-9	C_{3v}	Johnson triangular cupola J3	16.212
JCCU-9	C_{4v}	Capped cube J8	8.263
CCU-9	C_{4v}	Spherical-relaxed capped cube	6.640
JCSAPR-9	C_{4v}	Capped square antiprism J10	3.590
CSAPR-9	C_{4v}	Spherical capped square antiprism	2.839
JTCTPR-9	D_{3h}	Tricapped trigonal prism J51	4.314
TCTPR-9	D_{3h}	Spherical tricapped trigonal prism	2.462
JTDIC-9	C_{3v}	Tridiminished icosahedron J63	12.111

HH-9	C_{2v}	Hula-hoop	9.315
MFF-9	C_s	Muffin	2.689

Thermal analysis.

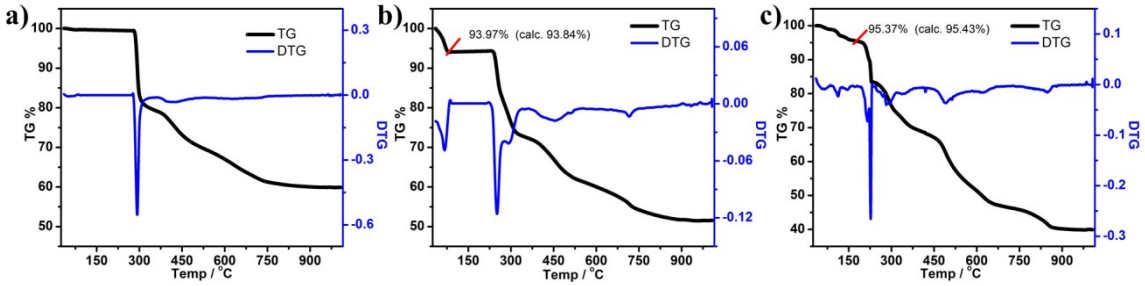

Figure S1. The TG curves of **1** (a), **2** (b) and **3** (c) under heating in flowing N_2 at 5 °C·min^{-1} over the temperature range of 35-1000 °C.

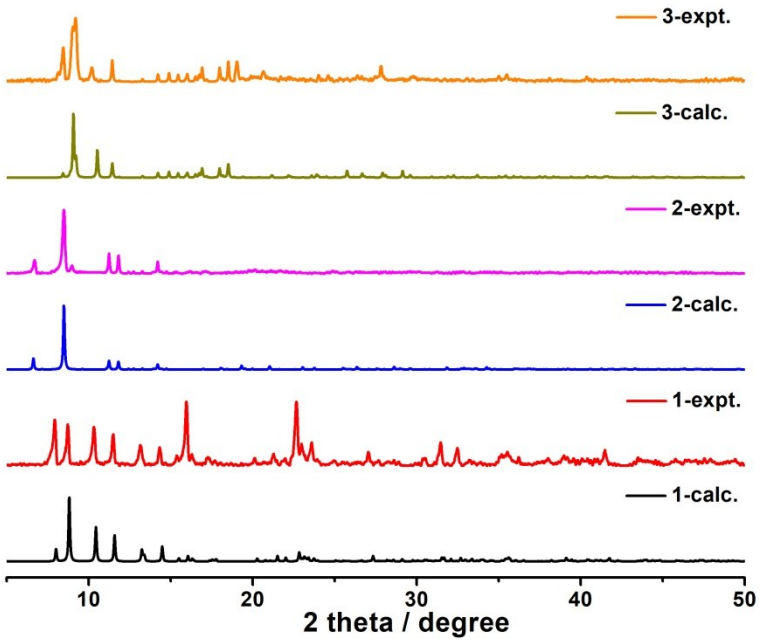

Figure S2. Powdered X-ray diffraction (XRD) patterns for complexes **1**, **2** and **3**.

Table S6. Major species assigned in the Time-dependent ESI-MS of **1** in positive mode.

m/z	Fragment	Relative Intensity									
		0min	10min	30min	1h	2h	3 h	6h	12	24h	48h
166.09	$[(\mathbf{L^1})+H]^+$(*calc.* 166.09)	1	1	1	0	0	0	0	0	0	0
337.09	$[Ni(\mathbf{L^1})(CH_3OH)(CH_3CN)_2]^+$(*calc.* 337.09)	0.027	0.052	0.120	0.355	0.309	0.390	0.594	0.750	0.234	0.116
342.02	$[Ni(H\mathbf{L^1})(NO_3)(H_2O)(CH_3CN)]^+$(*calc.* 342.02)	0.284	0.272	0.110	0.116	0.154	0.138	0.234	0.278	0.296	0.135
387.09	$[Ni(\mathbf{L^1})(H\mathbf{L^1})]^+$(*calc.* 387.09)	0.430	0.813	0.767	0.682	0.589	0.325	0.063	0.036	0.048	0
439.00	$[Dy(\mathbf{L^1})(NO_3)_2(CH_3OH)(H_2O)]^+$(*calc.* 439.02)	0	0	0.376	0.464	0.201	0.237	0.175	0.184	0.204	0.116
673.98	$[DyNi(\mathbf{L^1})_2(NO_3)_2]^+$(*calc.* 673.98)	0.195	0.403	0.748	1	1	1	0.732	0.540	0.421	0.256
777.05	$[DyNi(\mathbf{L^1})_3(NO_3)]^+$(*calc.* 777.07)	0.085	0.178	0.558	0.446	0.445	0.327	0.334	0.452	0.281	0.062
1408.00	$[Dy_2Ni_2(\mathbf{L^1})_4(CH_3O)_2(NO_3)_4+H]^+$(*calc.* 1408.00)	0	0.021	0.100	0.344	0.471	0.564	0.924	1	0.875	1
1451.07	$[Dy_2Ni_2(\mathbf{L^1})_4(CH_3O)(OH)(NO_3)_3(CH_3CN)_2(H_2O)_2]^+$(*calc.* 1451.07)	0	0.024	0.108	0.368	0.511	0.610	1	0.688	1	0.902

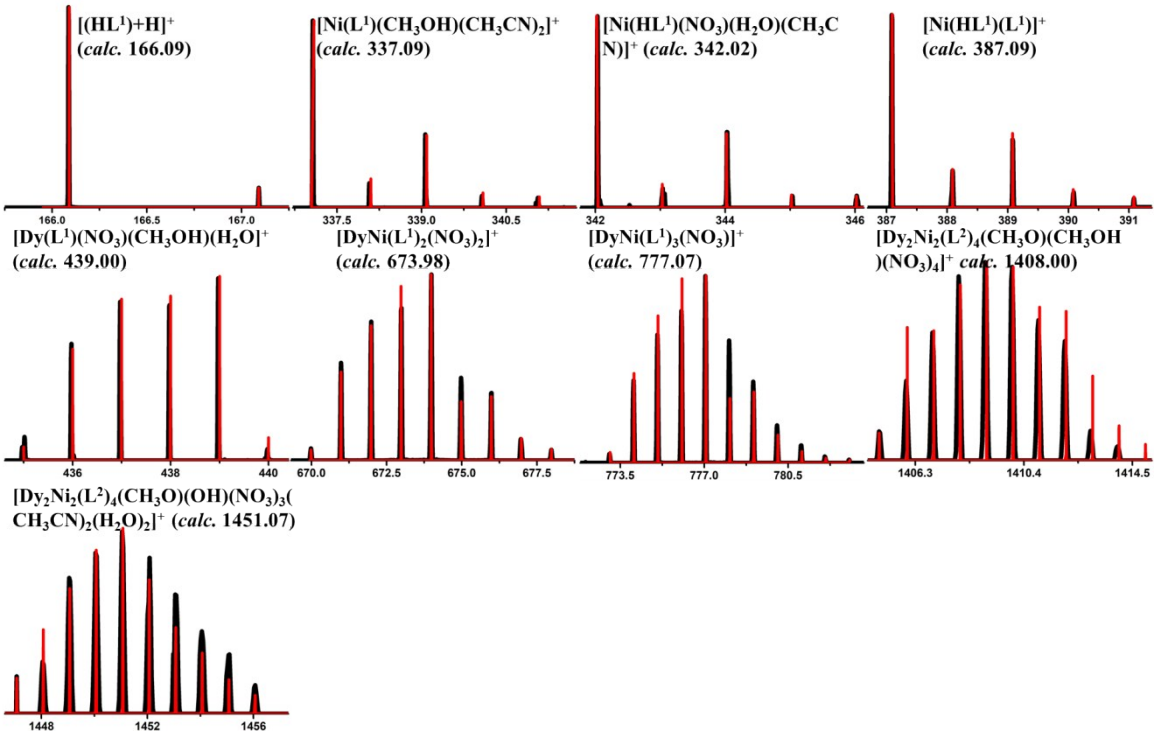

Figure S3. The superposed simulated and observed spectra of several species in the Time-dependent HRESI-MS of **1** (positive mode).

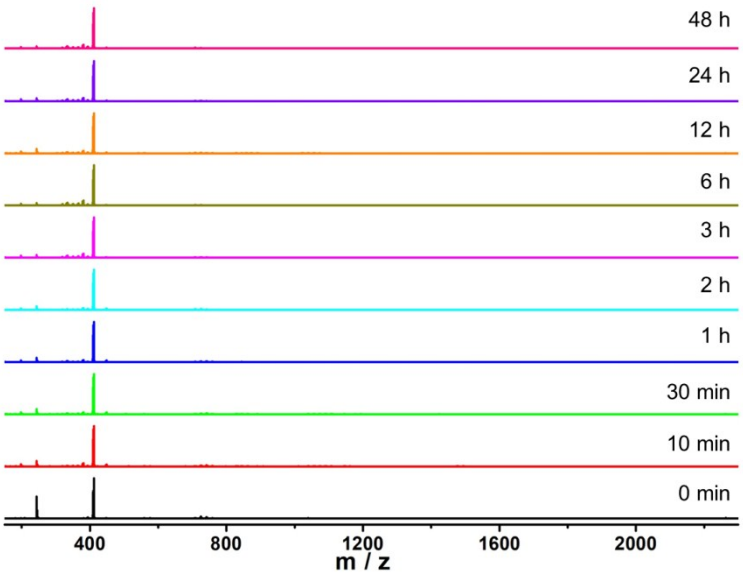

Figure S4. Time-dependent HRESI-MS spectra for stepwise assembly of **1** in a negative mode.

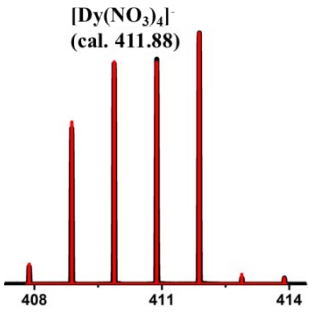

Figure S5. The superposed simulated and observed spectra of several species in the Time-dependent HRESI-MS of **1** (negative mode).

Table S7. Major species assigned in the Time-dependent HRESI-MS of **2** in positivemode.

m/z	Fragment	Relative Intensity									
		0min	10min	30min	1h	2h	3 h	6h	12	24h	48h
415.12	$[Ni(\mathbf{L^2})_2H]^+$(*calc.* 415.12)	1	1	0.802	0.475	0.650	0.519	0.454	0.315	0.231	0.532
702.01	$[DyNi(\mathbf{L^2})_2(NO_3)_2]^+$(*calc.* 702.01)	0.313	0.723	1	1	1	0.783	0.687	0.412	0.109	0.028
787.14	$[DyNi(\mathbf{L^2})_3(CH_3O)]^+$(*calc.* 787.14)	0	0	0	0	0	0.226	0.037	0	0	0
987.98	$[Dy_2Ni(\mathbf{L^2})_2(NO_3)_3(CH_3O)_2]^+$(*calc.* 987.97)	0	0	0.116	0.283	0.351	0.285	0.309	0.128	0.291	0.147
1001.01	$[Dy_2Ni(\mathbf{L^2})_2(NO_3)_2(CH_3O)(OH)_2(H_2O)_4]^+$(*calc.* 1001.00)	0	0	0.231	0.472	0.704	1	0.857	0.649	0.497	0.319
1152.95	$[Dy_2Ni(\mathbf{L^2})_2(NO_3)_5(CH_3OH)(H_2O)_4]^+$(*calc.* 1152.97)	0	0	0.047	0.082	0.099	0.170	0.189	0.118	0.163	0.033
1402.07	$[Dy_2Ni_2(\mathbf{L^2})_4(NO_3)_3(CH_3O)_2]^+$(*calc.* 1402.07)	0	0	0	0.027	0.334	0.773	1	1	1	1

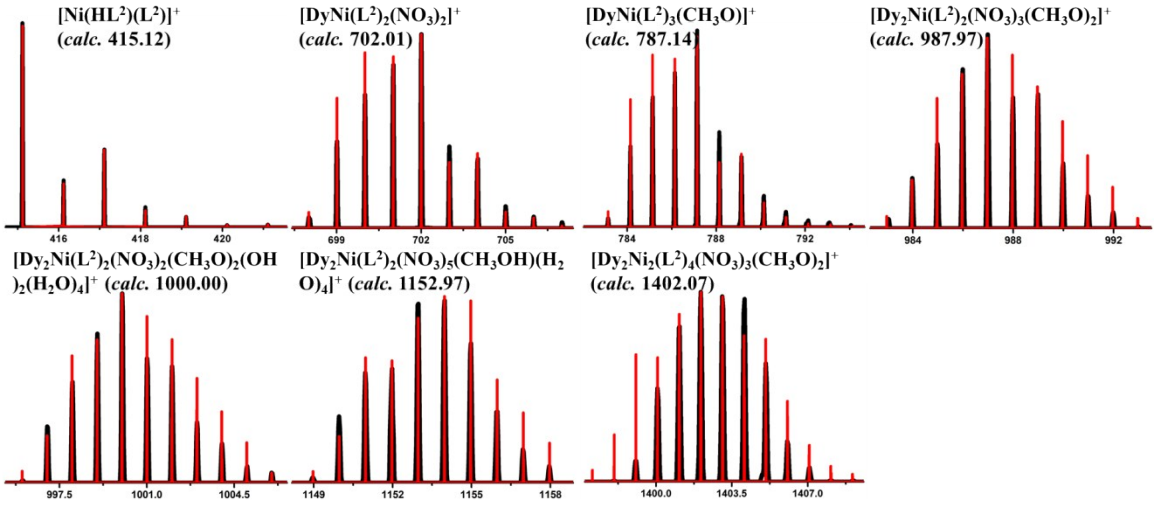

Figure S6. The superposed simulated and observed spectra of several species in the Time-dependent HRESI-MS of **2** (positive mode).

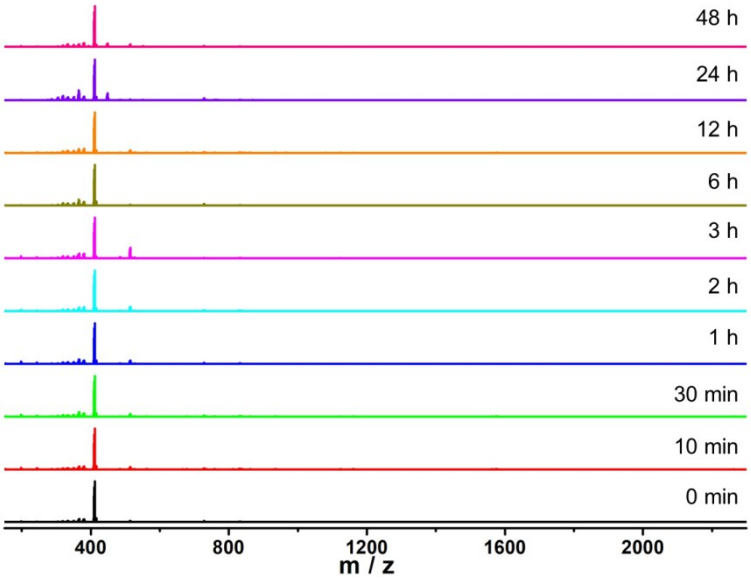

Figure S7a. Time-dependent HRESI-MS spectra for stepwise assembly of **2** in a negative mode.

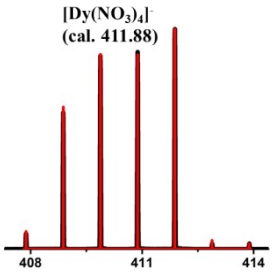

Figure S7b. The superposed simulated and observed spectra of several species in the Time-dependent HRESI-MS of **2** (negative mode).

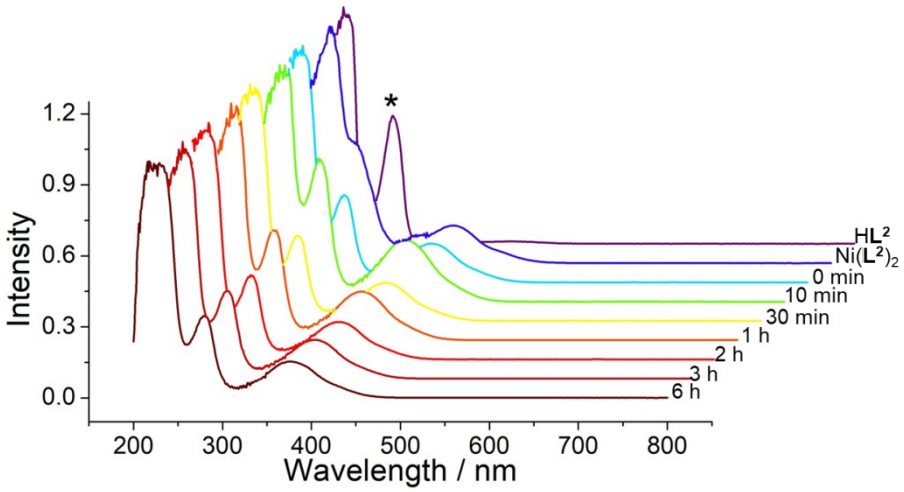

Figure S8. The reverse phenomenon in Ni($\mathbf{L^2}$)$_2$ by UV-Vis.

Table S8. Major species assigned in the Time-dependent HRESI-MS of **3** in positive mode.

m/z	Fragment	Relative Intensity									
		0min	10min	30min	1h	2h	3 h	6h	12	24h	48h
415.12	$[Ni(\mathbf{L^2})_2H]^+$(*calc.* 415.12)	1	1	1	0.882	0.706	0.461	0.259	0.097	0.022	0.011
437.10	$[NiNa(\mathbf{L^2})_2]^+$(*calc.* 437.10)	0.220	0.474	0.782	1	1	0.796	0.501	0.237	0.087	0.004
520.11	$[NiNa_2(\mathbf{L^2})_2(N_3)(H_2O)]^+$(*calc.* 520.11)	0.025	0.247	0.311	0.596	0.746	0.874	0.853	0.672	0.371	0.001
545.11	$[NiNa_2(\mathbf{L^2})_2(N_3)_2+H]^+$(*calc.* 545.11)	0.089	0.308	0.436	0.623	0.898	1	1	0.902	0.533	0.148
566.15	$[NiNa_2(\mathbf{L^2})_2(N_3)(CH_3OH)_2]^+$(*calc.* 566.15)	0.031	0.198	0.292	0.435	0.677	0.629	0.783	0.576	0.210	0.092
851.20	$[Ni_2Na(\mathbf{L^2})_4]^+$(*calc.* 851.21)	0	0	0.021	0.094	0.129	0.147	0.194	0.116	0.037	0.009
894.22	$[Ni_2Na(\mathbf{L^2})_4(N_3)+H]^+$(*calc.* 894.22)	0	0	0.077	0.126	0.185	0.224	0.197	0.163	0.114	0.028
959.21	$[Ni_2Na_2(\mathbf{L^2})_4(N_3)_2+H]^+$(*calc.* 959.22)	0	0	0.001	0.098	0.219	0.502	0.822	0.951	1	0.975
991.24	$[Ni_2Na_2(\mathbf{L^2})_4(N_3)_2(CH_3OH)+H]^+$(*calc.* 991.25)	0	0	0	0.068	0.154	0.381	0.763	0.905	0.927	0.896
1020.24	$[Ni_2Na_2(\mathbf{L^2})_4(N_3)_3(H_2O)+HH]^+$(*calc.* 1020.25)	0	0	0	0.040	0.176	0.327	0.804	1	0.984	1
1034.27	$[Ni_2Na_2(\mathbf{L^2})_4(N_3)_3(CH_3OH)+HH]^+$(*calc.* 1034.27)	0	0	0	0.027	0.166	0.292	0.713	0.918	0.946	0.890

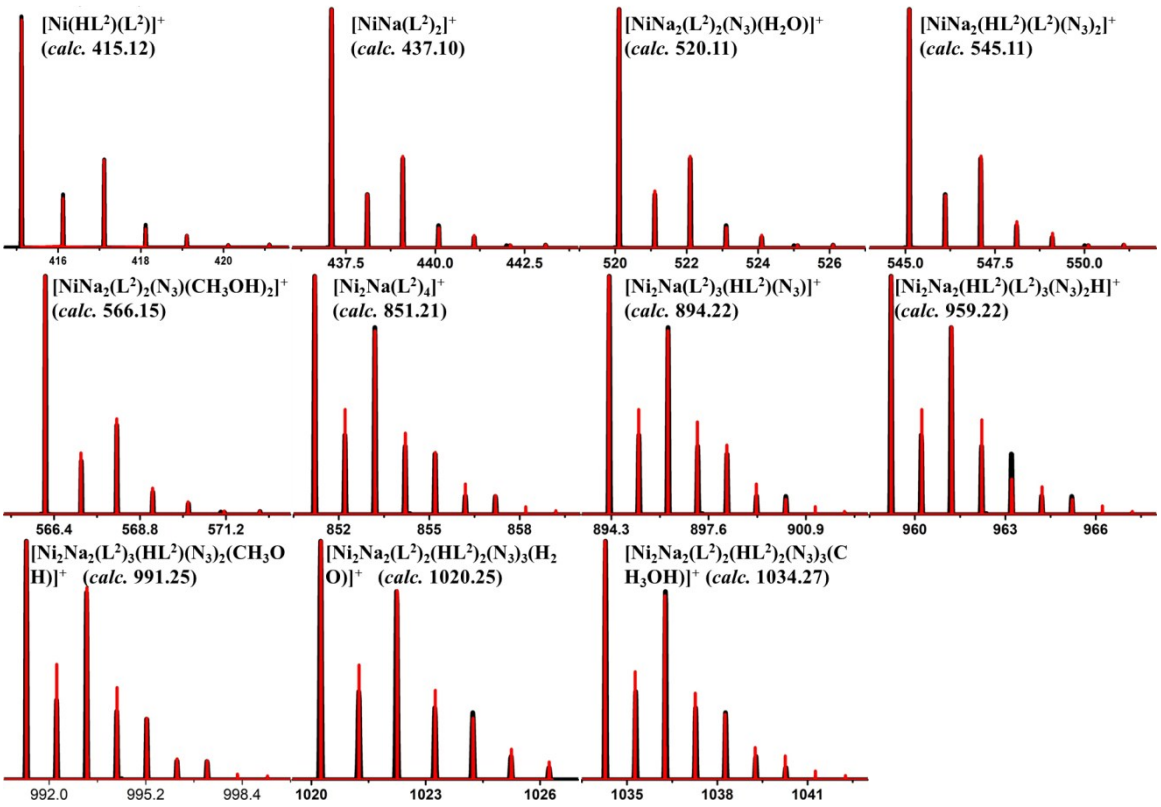

Figure S9. The superposed simulated and observed spectra of several species in the Time-dependent HRESI-MS of **3** (positive mode).

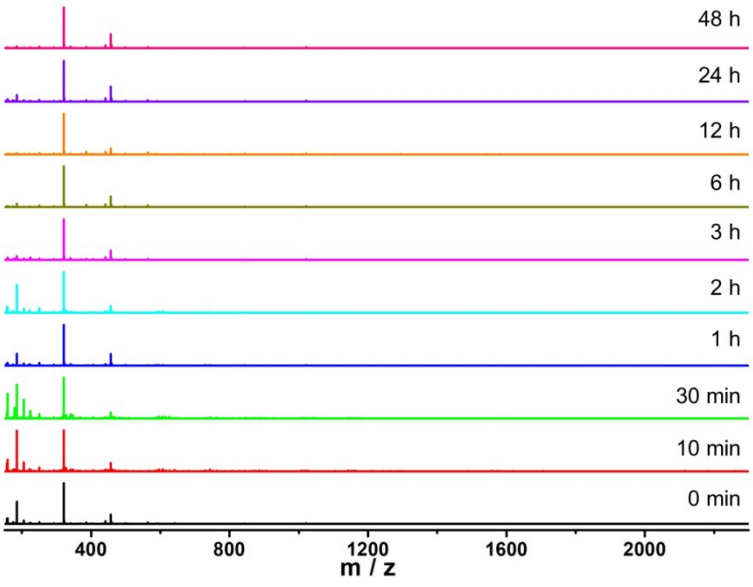

Figure S10. Time-dependent HRESI-MS spectra for stepwise assembly of **3** in a negative mode.

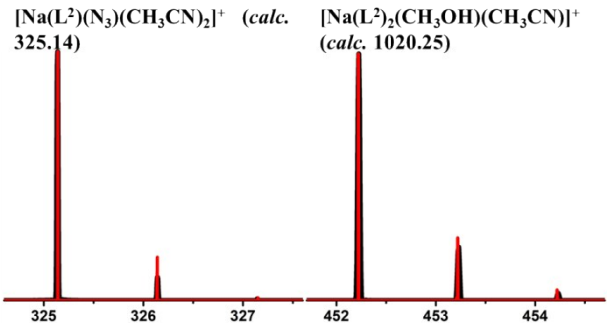

Figure S11. The superposed simulated and observed spectra of several species in the Time-dependent HRESI-MS of **3** (negative mode).

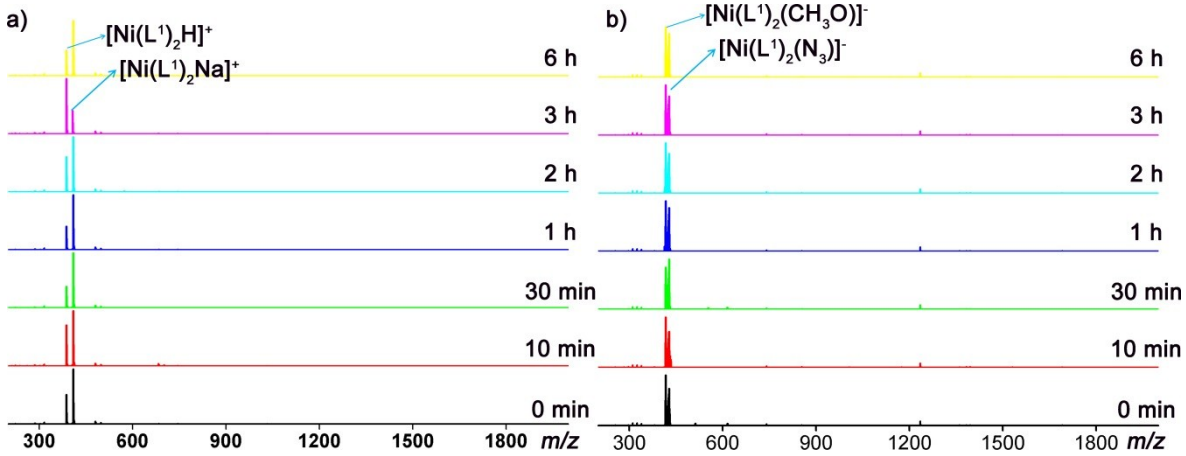

Figure S12. Time-dependent HRESI-MS tracks the reaction between Ni(**L**^{1})$_2$ and NaN_3: (a) positive mode; (b) negative mode.

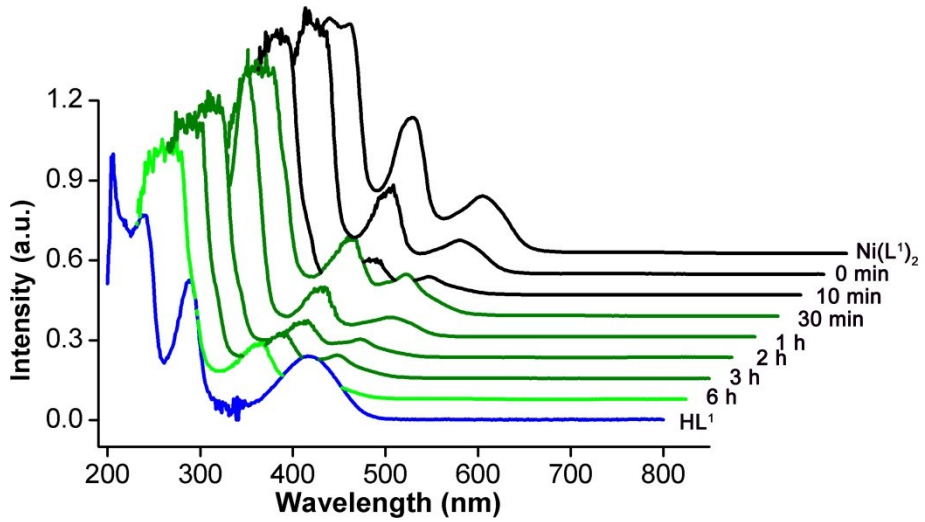

Figure S13. UV-Vis absorption spectroscopy tracks the reaction between Ni(**L**^{1})$_2$ and NaN_3.

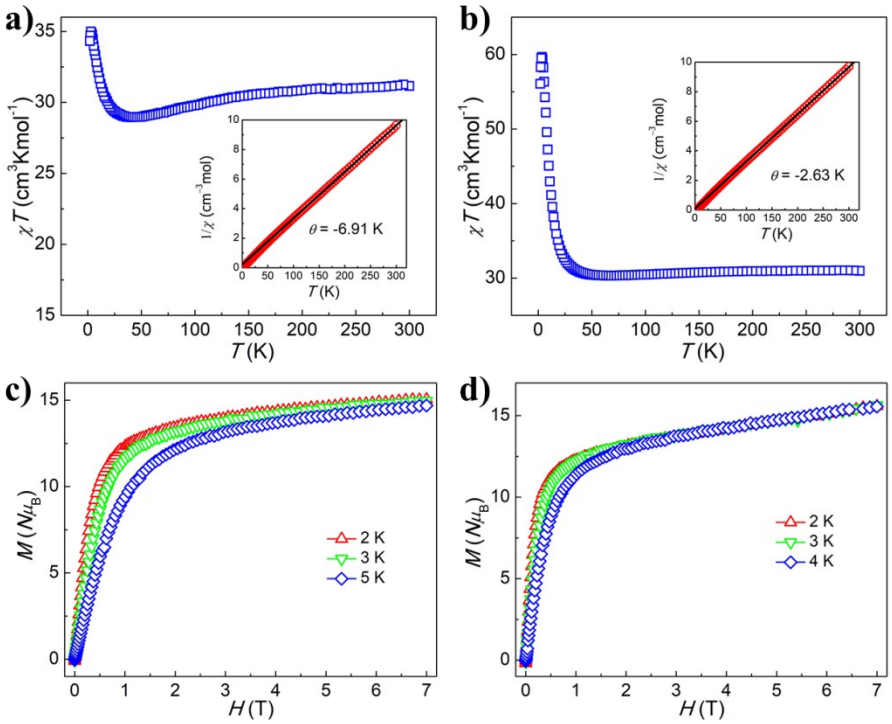

Figure S14. Temperature dependence of $\chi_m T$ and θ of $1/\chi$ for **1** (a) and **2** (b); *M* vs. *H*/*T* plots for **1** (c) and **2** (d)**.**

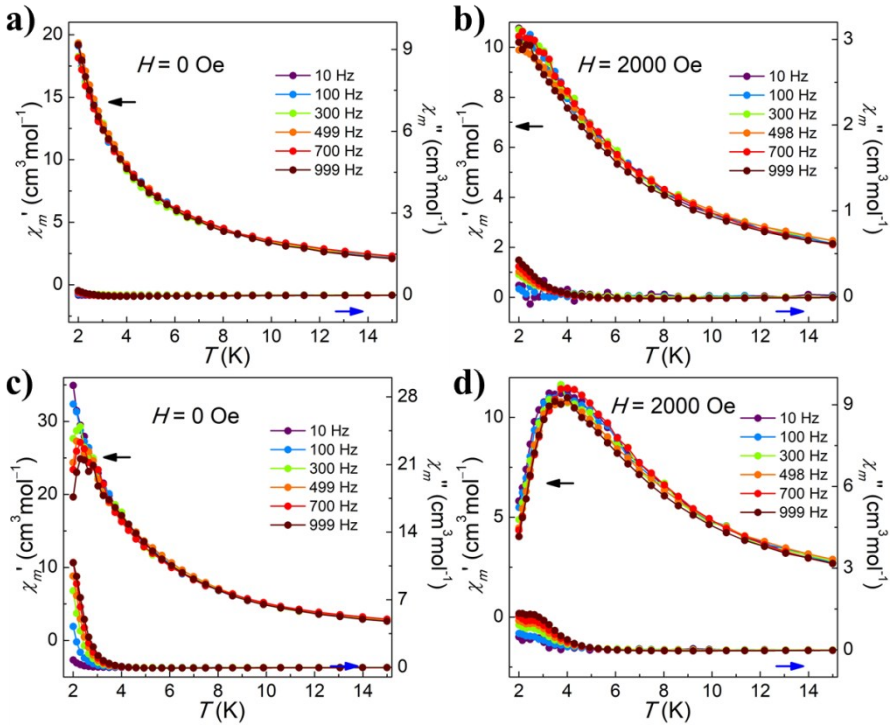

Figure S15. The temperature dependence of the in-phase (χ') and out-of-phase (χ'') ac-susceptibilities for different frequencies in a zero dc-field and 2000 Oe dc-field for **1** (a, b) and **2** (c, d).